

RESEARCH

Open Access



# Semaphorin 7a is protective through immune modulation during acetaminophen-induced liver injury

Eilidh J. Livingstone<sup>1†</sup>, Jennifer A. Cartwright<sup>2,3\*†</sup>, Lara Campana<sup>1</sup>, Philip J. Starkey Lewis<sup>1</sup>, Benjamin J. Dwyer<sup>1</sup>, Rhona Aird<sup>1</sup>, Tak Yung Man<sup>1</sup>, Matthieu Vermeren<sup>1</sup>, Adriano Giorgio Rossi<sup>2</sup>, Luke Boulter<sup>4</sup> and Stuart John Forbes<sup>1</sup>

## Abstract

**Background and Aim** Acetaminophen (APAP) induced acute liver injury (ALI), the leading cause acute liver failure in the western world, has limited treatment options. APAP toxicity results in massive hepatic necrosis and secondary infiltrating monocytes and neutrophils, which contribute to pathogenesis. Semaphorin 7a (Sema7a), a chemoattractant and modulator of monocytes and neutrophils, is a potential therapeutic target in other conditions, but its role in APAP-ALI is unexplored.

**Methods** Wild-type (WT) and Sema7a knockout (KO) mice were examined during APAP-ALI. Serum liver function tests, histological analysis and cellular localisation of Sema7a and its receptors, Plexin C1 and Integrin  $\beta$ 1, were examined. Serum cytokines were quantified, tissue macrophages and neutrophils were localised, and in vivo phenotype, including phagocytosis, was assessed by immunohistochemistry and flow cytometry.

**Results** Sema7a was expressed by HNF4 $\alpha$  + peri-necrotic hepatocytes circumferentially during APAP-ALI injury phases, and serum concentrations were increased, and correlated with hepatic injury. Sema7a KO mice had increased circulating inflammatory cytokines and significantly less hepatic F4/80 + macrophages, a cell type required for hepatic repair. Sema7a KO mice had higher necrotic area neutrophils, and increased neutrophil chemoattractant CXCL1. Without Sema7a expression, mice displayed increased necrosis and liver injury markers compared to Sema7a WT mice. Without peri-necrotic hepatocyte Sema7a expression, we also identified increased cell death and hepatic cellular stress outside of necrosis.

**Conclusion** We have identified a novel protective role of Sema7a during injury phases of APAP-ALI. Without peri-necrotic hepatocyte Sema7a expression and secretion, there is increased inflammation, time specific worsened hepatic necrosis and increased hepatic cell stress and death outside of the necrotic zone.

**Keywords** Sema7a, Paracetamol, APAP, APAP-induced liver injury, Macrophages, Neutrophils

<sup>†</sup>Eilidh J. Livingstone and Jennifer Ann Cartwright Joint first author.

\*Correspondence:

Jennifer A. Cartwright

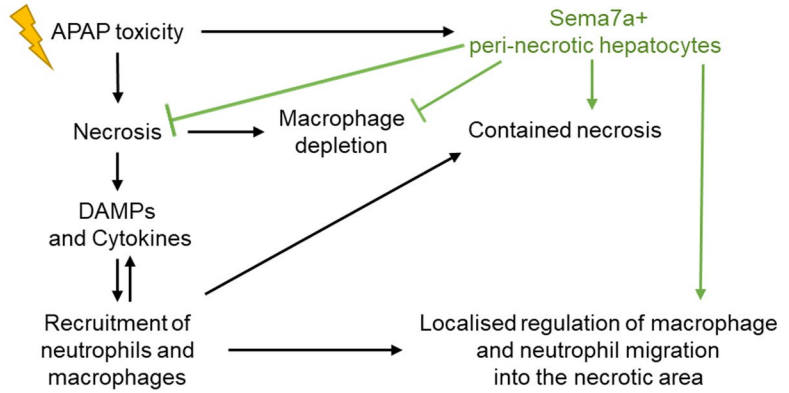
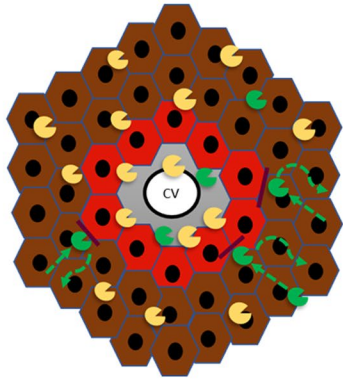
Jennifer.cartwright@ed.ac.uk

Full list of author information is available at the end of the article

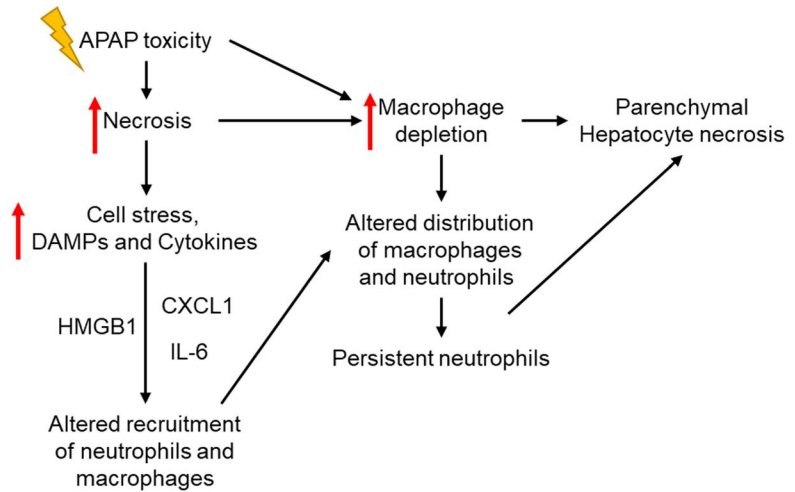
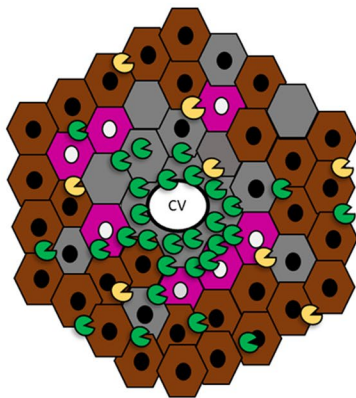


**Graphical Abstract**

**WT mice:**



**Sema7a KO mice:**



-  F4/80+ Macrophage
-  Ly6G+ Neutrophil
-  Healthy hepatocyte
-  Sema7a+ hepatocyte
-  Dying hepatocyte
-  Hepatocyte releasing HMGB1

## Synopsis

Semaphorin 7a (Sema7a) is expressed on hepatocytes in a circular ring surrounding necrotic cells during acute liver injury, and circulatory levels correlate with damage. Without peri-necrotic Sema7a and secretion, there is increased hepatic inflammation, and worsened necrosis, cell stress and death.

## Background

Acetaminophen (APAP) is a widely used analgesic and antipyretic medication, which is safe at therapeutic doses but overdose causes 46% of acute liver failure (ALF) in Western countries, and it remains the commonest cause of ALF-induced death [1–3]. APAP-induced acute liver injury (APAP-ALI) causes systemic inflammation, which can lead to multiorgan dysfunction and sepsis [4, 5]. The current pharmacological therapy for APAP-ALI, N-acetylcysteine (NAC), is effective if given within 10 h of APAP overdose ingestion [6]. Otherwise, only supportive care is available. Liver transplantation is considered for patients that develop liver failure, but suitable donor organs are not always available [7, 8]. Therefore, alternative therapeutic strategies are required to limit hepatic injury and promote recovery. One potential therapeutic avenue is to manipulate the innate immune system to limit damage and promote tissue recovery.

Semaphorins are a diverse family of highly conserved signalling proteins, that perform a variety of functions from neurogenesis axon guidance to bone homeostasis and immune responses [9–12]. Semaphorin 7a (Sema7a) is an immune semaphorin that modulates immune processes such as inflammatory infiltration, immune cell interactions, activation and suppression [10, 13, 14]. Sema7a is the only semaphorin connected to the membrane via a glycosylphosphatidylinositol linker, and it is expressed by neurones, immune cells and activated hepatic stellate cells [9, 15, 16]. Sema7a has two receptors Integrin  $\beta 1$  and Plexin C1 [17, 18], and promotes immune cell migration, such as facilitating neutrophil pulmonary transmigration [18, 19], or acting as a chemoattractant for monocytes and macrophages [20, 21]. Sema7a has cumulative evidence for involvement in auto-immune and inflammatory diseases [15, 20, 22] and anti-Sema7a treatment has shown efficacy for some of these conditions [23, 24]. More recent reports indicate a role in reducing inflammation in acute tissue damage [25, 26] but its actions have not been evaluated in APAP-ALI.

Despite conflicting literature, there is now substantial evidence that macrophages play a key role in resolving injury and inflammation following ALI [27–30], with poor outcomes from APAP-ALI correlating with blood monocytopenia [31]. Macrophages are highly plastic cells which acquire distinct phenotypes depending

on molecular cues in their microenvironment [32, 33]. Ly6C<sup>hi</sup> macrophages show a pro-inflammatory phenotype, whereas Ly6C<sup>lo</sup> macrophages are considered restorative and promote restoration of the liver after CCl<sub>4</sub> injury [34]. Sema7a can influence macrophage behaviour in a receptor-dependent manner and both pro-reparative and proinflammatory phenotypes have been documented [15, 22, 26].

APAP-ALI causes hepatocyte necrosis and the release of danger-associated-molecular patterns (DAMPs). DAMPs activate Kupffer cells (KCs), the liver resident macrophage, to release cytokines, which activate the innate immune system. This causes monocytes, macrophages and neutrophils to infiltrate the liver [33]. During APAP-ALI, KCs are depleted and monocyte-derived macrophages infiltrate the liver in large numbers [32]. Restorative Ly6C<sup>lo</sup> macrophages have been shown to be crucial for appropriate liver repair via phagocytosis [35, 36] and secretion of IL-10 to reduce inflammation [28]. Macrophage ablation delays repair [29, 32, 37] and stimulating macrophage proliferation, or delivering alternatively-activated macrophages can promote liver regeneration [38, 39]. Neutrophils have controversial roles in APAP-ALI, with reports indicating they contribute to injury, or tissue repair [40–44]. Since Sema7a influences macrophage phenotype and has involvements in neutrophil migration, we tested whether Sema7a has a hepatoprotective role during acute liver injury and repair.

Using a genetic ablation approach, we describe the local and temporal effects of Sema7a during APAP-ALI, detailing Sema7a expression on peri-necrotic hepatocytes during injury and repair, and its importance to limit hepatocyte damage and reduce inflammation. We report that Sema7a KO mice have reduced hepatic F4/80+ macrophages, higher numbers of neutrophils within necrotic areas, and increased pro-inflammatory serum cytokine concentrations, alongside increased spread of tissue damage. In conclusion, we report that Sema7a has a protective role in APAP-ALI and modulates innate immune cells to limit the damage caused by APAP-ALI.

## Methods

All authors had access to the study data and had reviewed and approved the final manuscript.

### In vivo experiments

#### Animals

C57BL/6J or Sema7a<sup>-/-</sup> mice (Jackson Laboratory, C57BL/6J background) were housed in specific pathogen-free environment and kept under standard conditions with a 12 h day/night cycle and access to food and water ad libitum. Mouse genotyping was performed by a commercial laboratory (Transnetyx). All animal

experiments were carried out under procedural guidelines, severity protocols and with ethical permission from the University of Edinburgh Animal Welfare and Ethical Review Body and the Home Office (UK), licence numbers 70/7847 and P231C5F81.

#### **APAP experiments**

9–12 week old male mice were fasted for 12 h then intra-peritoneally (i.p.) injected with 350 mg/kg APAP (Sigma), dissolved in sterile saline,  $n \geq 6$  / group. Controls were injected with an equivalent volume of sterile saline. Mice were kept in a 28 °C heat box, and closely monitored for the duration of the experiment.

Mice were humanely euthanised and blood was collected by cardiac puncture, into EDTA tubes for flow cytometry analysis, or clotted overnight at 4 °C then centrifuged for 10 min,  $8,000 \times g$  at 4 °C and serum collected. Livers were perfused with PBS and snap frozen or fixed in formalin overnight and paraffin embedded (FFPE).

Non-haemolysed serum liver function tests (LFTs) were performed by Dr Forbes Howie at the QMRI, University of Edinburgh according to manufacturer instructions (Alpha Laboratories). Kit instruction were adapted for use in the Cobas Fara or Cobas Mira analyser (Roche).

#### **Immunohistochemistry**

Frozen sections were fixed for 20 min with ice cold Methanol: Acetone. 4  $\mu\text{m}$ -thick FFPE sections were dewaxed and rehydrated before 15 min heat mediated antigen retrieval then permeabilised in PBS 0.1% Tween 20 (PBST). For IF sections were blocked for 30 min at RT with Protein Block (Spring Bio), then incubated overnight with the primary antibody at 4 °C, then incubated with secondary antibodies for 1 h RT. Sections were stained with DAPI (1:1,000) and mounted with fluoromount (Southern Biotech).

For 3,3'-diaminobenzidine (DAB) stains, FFPE sections were sequentially blocked at RT with Bloxall (Vector) for 15 min, then Avidin and Biotin (Invitrogen) for 10 min each, followed by 30 min Protein Block. Sections were stained overnight at 4 °C with the primary antibody, followed by the secondary antibody for 1 h at RT. Slides were blocked with R.T.U. VECTASTAIN Elite ABC reagent (Vector) for 30 min, before detection with DAB (DAKO). Slides were counterstained with haematoxylin before dehydration and mounting. All primary antibodies, their required antigen retrieval and dilution is provided in Supplementary Table 1 & 2. Isotype controls can be seen in Supplementary Fig. 1, Supplementary Materials & Methods Figs. 1 and 2.

Haematoxylin and Eosin (H&E) staining and block processing was performed by SuRF Histology at the QMRI, University of Edinburgh. Slides were scanned with the

Vectra Polaris multispectral slide scanner, and necrotic areas were segmented and quantified using inForm 2.4 (Perkin Elmer) software after tissue specific training, using eight  $10 \times \text{FOV}$  per mouse liver, at 1  $\mu\text{m}$  resolution, as shown in Supplementary Materials & Methods Fig. 3.

#### **Microscopy and image analysis**

Fluorescent and brightfield images were acquired using a Nikon Eclipse e600 microscope fitted with a Retiga 2000R camera (Q-Imaging, Image Pro premier software). Images were contrasted and analysed using Fiji ImageJ (ImageJ version 1.52e software for Windows (ImageJ Software, National Institutes of Health, USA, available at: <http://rsb.info.nih.gov/ij/>)). The isotype control acted as the negative reference. All images from one batch of staining were treated equally.

Numbers of Ly6G+ cells were counted manually on at least five  $10 \times \text{FOV}$  per slide. Number of F4/80+ cells were quantified using a macroinstruction on six  $20 \times \text{FOV}$  per slide. Number of Ly6G+ or F4/80+ cells were divided by the necrotic area of the respective slide to give number of cells per necrotic area. Separation of the inner and outer necrotic area is demonstrated in Supplementary Materials & Methods Fig. 5. Percentage area of Sema7a positivity on DAB staining was quantified using a Fiji image J macroinstruction on six  $20 \times \text{FOV}$  per slide.

Confocal microscopy was performed with an inverted Leica TCS SP8 Confocal microscope. High magnification images used the Nyquist criterion to give the maximum resolution using  $60 \times$  objective lens. Images were converted from Z- stacks to Maximum Intensity Projections, and contrast adjusted using Fiji ImageJ.

#### **TUNEL assay**

Terminal deoxynucleotidyl transferase-mediated biotinylated deoxy-uridine triphosphate nickend labelling (TUNEL) assay, was performed on 4  $\mu\text{m}$  FFPE tissue according to manufacturer instructions (In Situ Cell Death Detection Kit, TMR Red, Roche). TUNEL+DAPI+nuclei were imaged and quantified using the Perkin Elmer Operetta high content imaging system and Columbus software (Supplementary Materials & Methods Fig. 4).

#### **Protein quantification**

##### **Protein extraction**

60 mg liver tissue was homogenised with a Tissue Tearor (Biospec Products) in cold Meso Scale Diagnostics (MSD) lysis buffer (150 mM NaCl, 20 mM Tris pH7.5, 1 mM EGTA, 1 mM EDTA, 1% Triton X-100, 1X Halt Protease inhibitor Cocktail (Thermo Scientific)). Homogenates were slowly mixed for 30 min, then centrifuged for 10 min  $20,000 \times g$  at 4 °C. The aqueous



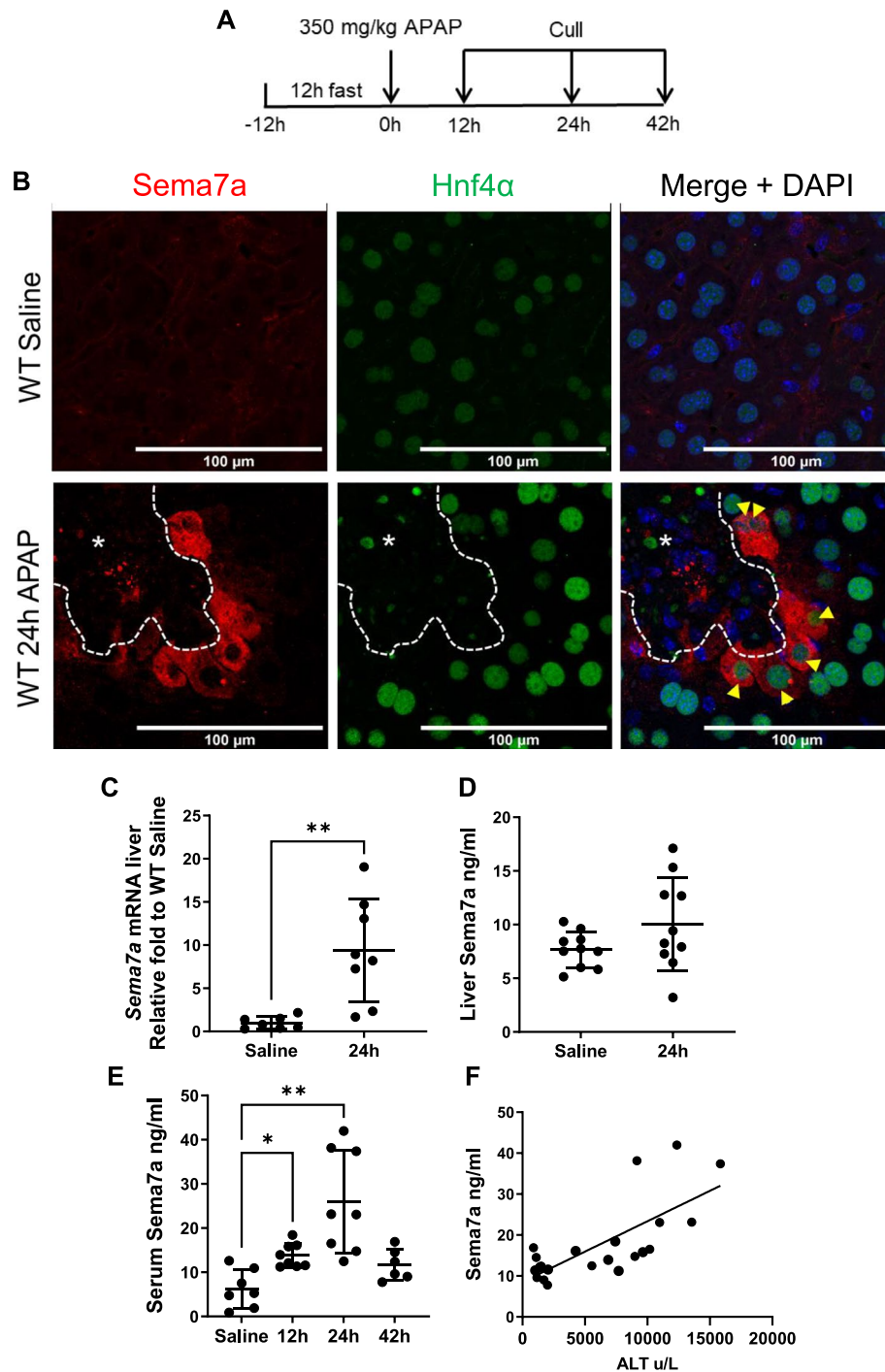


**Fig. 2** Sema7a is expressed by hepatocytes and correlates with serum ALT activity (A) Experimental schematic; WT mice received 350 mg/kg APAP i.p and tissues collected during injury (12 and 24 h) and repair (42 h) (B) Representative immunofluorescent labelled hepatic sections, Sema7a (red) and Hnf4α (green) from healthy mice (top) and at 24 h APAP-ALI (bottom). Yellow arrows, Sema7a + Hnf4α + hepatocytes. White dashed line and \* indicate necrotic areas. C Whole liver lysate expression of Sema7a qRT-PCR, t-test, Welch's correction ( $p=0.0053$ ); and (D) ELISA, unpaired t-test ( $p=0.13$ ). E Sema7a ELISA on serum during an APAP-ALI time course, Brown-Forsythe ANOVA ( $P=0.0007$ ), Dunnett's comparisons Saline vs 12 h ( $p=0.0149$ ), Saline vs 24 h ( $p=0.0089$ ). F Correlation of Sema7a levels and ALT in serum. Linear Regression  $R^2=0.53$ ,  $P=0.0001$ . Scale bars 100 μm. Each datapoint represents an individual mouse. \*  $p < 0.05$ ; \*\*  $p < 0.01$ .  $n \geq 6$  mice/ time point

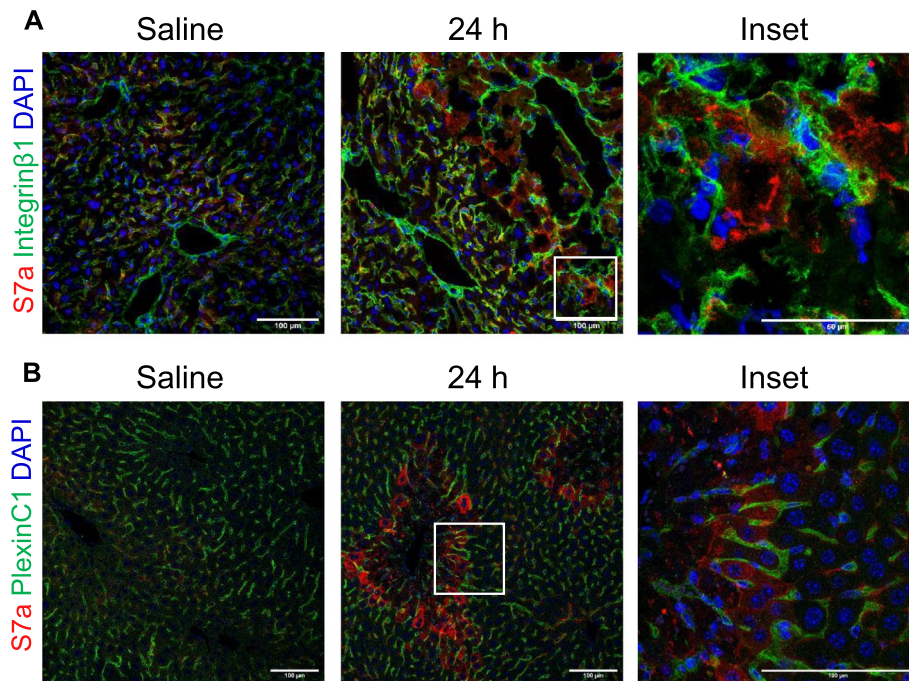


**Fig. 3** Expression of Sema7a and its Receptors PlexinC1 and Integrin  $\beta$ 1 Results from 24 h post 350 mg/kg APAP or saline treated WT mice, Scale bars 100  $\mu$ m. DAPI counterstain,  $n \geq 8$  mice/group, **(A)** Representative immunofluorescent labelled hepatic sections Sema7a (red) and Integrin  $\beta$ 1 (green) with insert showing proximity of cell to cell expression, but no colocalization. **B** Representative immunofluorescent labelled hepatic sections Sema7a (red) and Plexin C1 (green) with insert showing proximity of cell to cell expression, but no colocalization

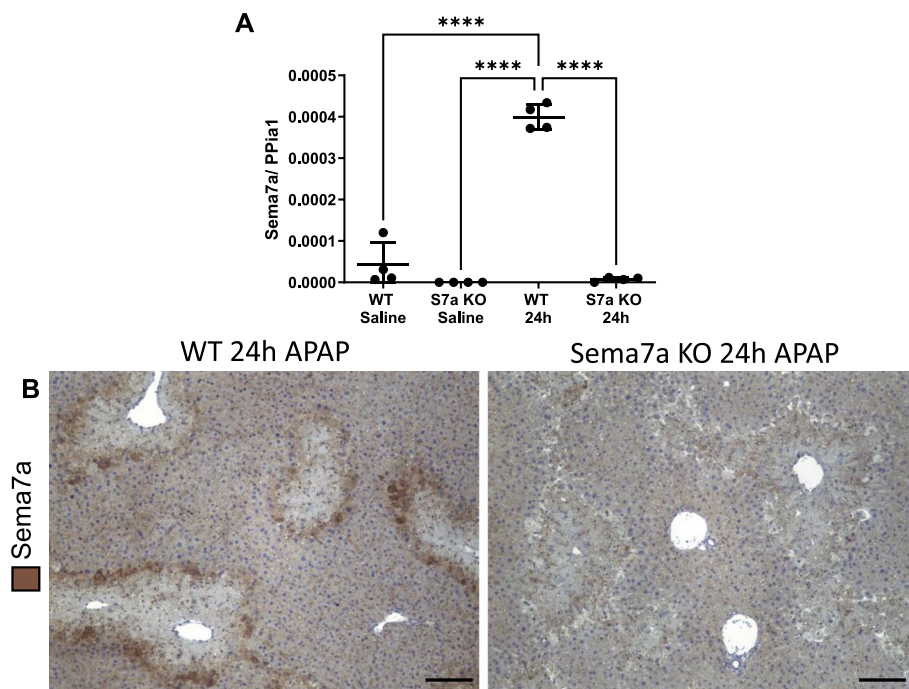


**Fig. 4** Sema7a KO mice do not express Sema7a Results from WT and Sema7A KO mice 24 h post saline or 350 mg/kg APAP. **A** Hepatic lysate qPCR, Sema7a mRNA expression relative to housekeeper PPIa1. WT APAP-ALI treated mice have significantly elevated expression at 24 h post APAP compared to all other groups (ANOVA,  $p < 0.0001$ , Tukey's multiple comparisons,  $p \leq 0.0001$ ).  $n = 4$ . **B** Representative hepatic Sema7a (DAB) labelled sections from WT and Sema7a mice 24 h post APAP, showing no expression in WT mice

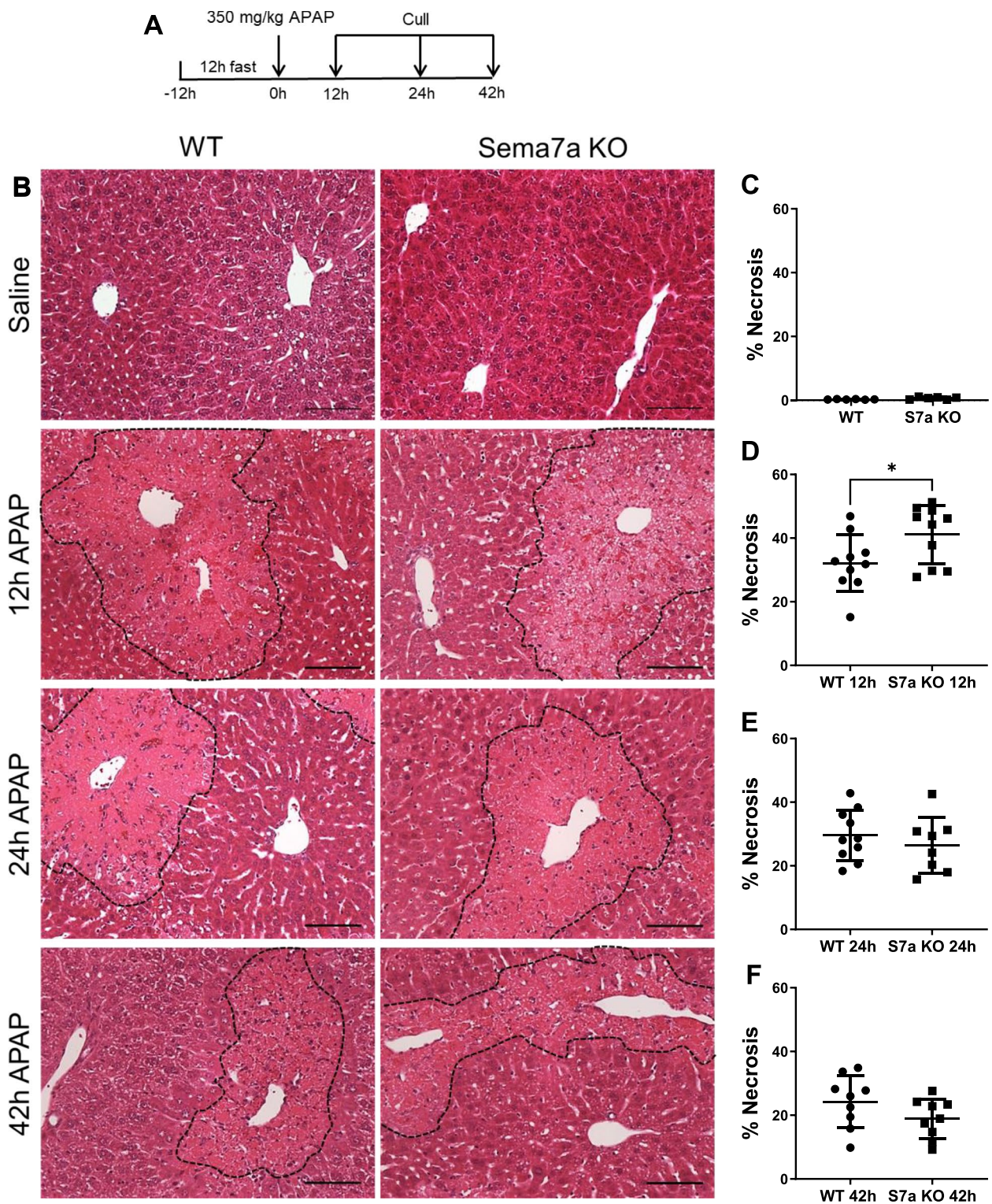


**Fig. 5** Sema7a KO mice have more liver necrosis during APAP-ALI. **A** Experimental schematic; WT and Sema7a KO mice treated with 350 mg/kg APAP, assessed at 12, 24 and 42 h. **B** Representative liver histological stains from Sema7a WT, and Sema7a KO mice. Necrotic areas outlined with black dashed line. Scale bars 100  $\mu$ m. **C-F** Necrosis quantification, necrotic areas were segmented and quantified using inForm 2.4 (Perkin Elmer) software using inform tissue training for consistent changes; enlarged cell organelles, membrane rupture and cell lysis at 0 h (**C**) 12 h, t-test ( $p=0.0391$ ) (**D**), 24 h (**E**) and 42 h (**F**) post 350 mg/kg APAP injection. Each datapoint represents a mouse. \*  $p < 0.05$ ; \*\*  $p < 0.01$ ,  $n \geq 8$  mice/group

serum using the V-PLEX Pro-inflammatory Panel 1' mouse plate (MSD), following the manufacturer instructions.

The plate was read on the QuickPlex SQ 120 analyser (MSD). Standard curves were used to quantify the concentration of the respective cytokine.

#### **Sema7a enzyme-linked immunosorbent assay (ELISA)**

The Mouse LS Bio sandwich ELISA kit was used to quantify Sema7a in mouse liver protein homogenate, diluted to 0.5 mg/ml, or mouse serum, diluted 1:5. Samples were diluted in sample diluent and assayed in duplicate by following the manufacturer's instructions (Manufacturer; LS-F6958).

#### **Quantitative reverse transcriptase PCR (qRT-PCR)**

40 mg of liver tissue was homogenised in 500  $\mu$ L Qiazol (Qiagen). Homogenates were mixed with 100  $\mu$ L chloroform, incubated at RT for 3 min, and then centrifuged at 4  $^{\circ}$ C 1200 $\times$ g, for 15 min. The aqueous supernatant was removed and mixed in an equal volume of 70% ethanol. RNA was extracted using an RNAeasy Kit according to manufacturer instructions (Qiagen). Reverse Transcription and Real Time-qPCR was performed using Qiagen Quantitect and Quantifast reagents on a LightCycler 480 II (Roche). Commercial primers (*peptidylprolyl isomerase A (PPIA)*, *Sema7a*, QT00173488) from Qiagen's Quantitect range were used. Gene expression was normalised to the housekeeping gene *PPIA*. Samples were run in technical triplicate.

#### **Statistics**

GraphPad Prism 8 Software was used for all statistical analysis. Data are presented as mean  $\pm$  SD. Each data-point represents a mouse. Normality was determined by

a Shapiro-Wilks test. To test two sample groups a two-tailed unpaired t-test, with a Welch correction applied if required, or Mann Whitney test was used to compare parametric or non-parametric data respectively. Sample size was based on a power calculation where  $\alpha=0.05$ , desired power = 0.8, or from investigator experience.

For further information on flow cytometry, imaging, and other materials and methods, please refer to the CTAT table and supplementary materials and methods.

## **Results**

### **Sema7a is expressed in peri-necrotic hepatocytes during APAP-ALI**

Sema7a protein expression, assessed by immunostaining during a time course of APAP-ALI, (Fig. 1A and Supplementary Fig. 1) was not detected in healthy liver tissue or during the early stages of APAP-ALI (0–8 h). As hepatic necrosis and inflammation progressed from 12 to 24 h post APAP-ALI, Sema7a expression was localised to peri-necrotic cells, with peak expression at 24 h post-APAP-ALI. Sema7a expression diminished as necrosis resolved (36–60 h post APAP-ALI) (Fig. 1B, C).

Since peak Sema7a expression occurs at 24 h post-APAP, we further characterised Sema7a expression at this time point. Sema7a/Hnf4 $\alpha$  dual staining identified that peri-necrotic hepatocytes express Sema7a (Fig. 2A). In perfused whole liver, *Sema7a* mRNA expression significantly increased with APAP-ALI compared to healthy mice ( $p=0.0053$ , Fig. 2B). However, hepatic Sema7a protein levels did not significantly change (Fig. 2C). This total hepatic difference between transcribed and translated quantification may reflect release of the protein into circulation. Circulating Sema7a significantly increased in mouse serum at 12 and 24 h post-APAP ( $p=0.0127$  and

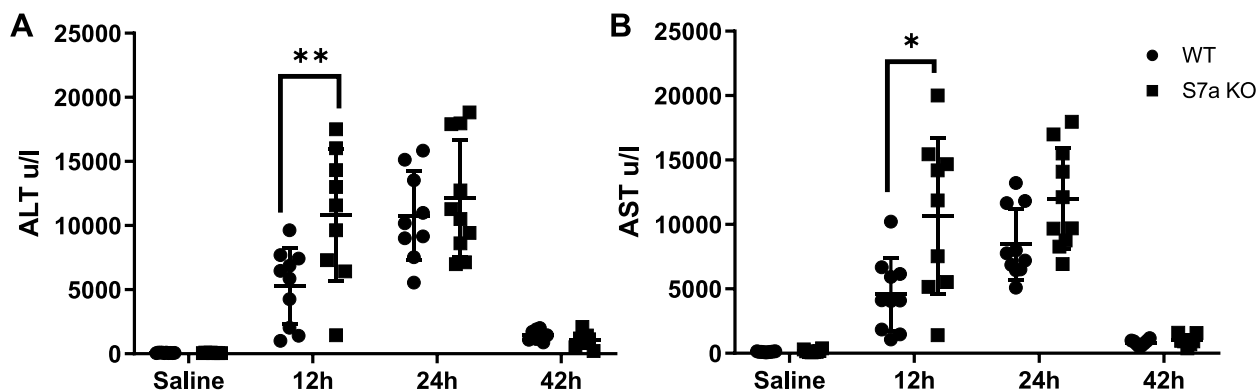


**Fig. 6** Sema7a KO mice have more liver damage during APAP-ALI. Serum markers of liver injury (LFTs), ALT (A) and AST (B) were higher at 12 h post 350 mg/kg APAP in Sema7a KO mice compared to WT mice during the time course of APAP-ALI, (t-test, Welch's correction,  $p=0.0095$  and  $p=0.0107$  respectively). Each datapoint represents a mouse. \*  $p < 0.05$ ; \*\*  $p < 0.01$ ,  $n \geq 7$  mice/group. During recovery, at 42 h post APAP-ALI, Sema7a KO mice and Sema7a WT mice exhibited similar necrosis (Fig. 5F) and proliferation (Supplementary Fig. 6). This suggests Sema7a does not directly influence recovery from APAP-ALI. However, Sema7a KO mice had raised ALP at this time point ( $p=0.0306$ , Supplementary Fig. 5)

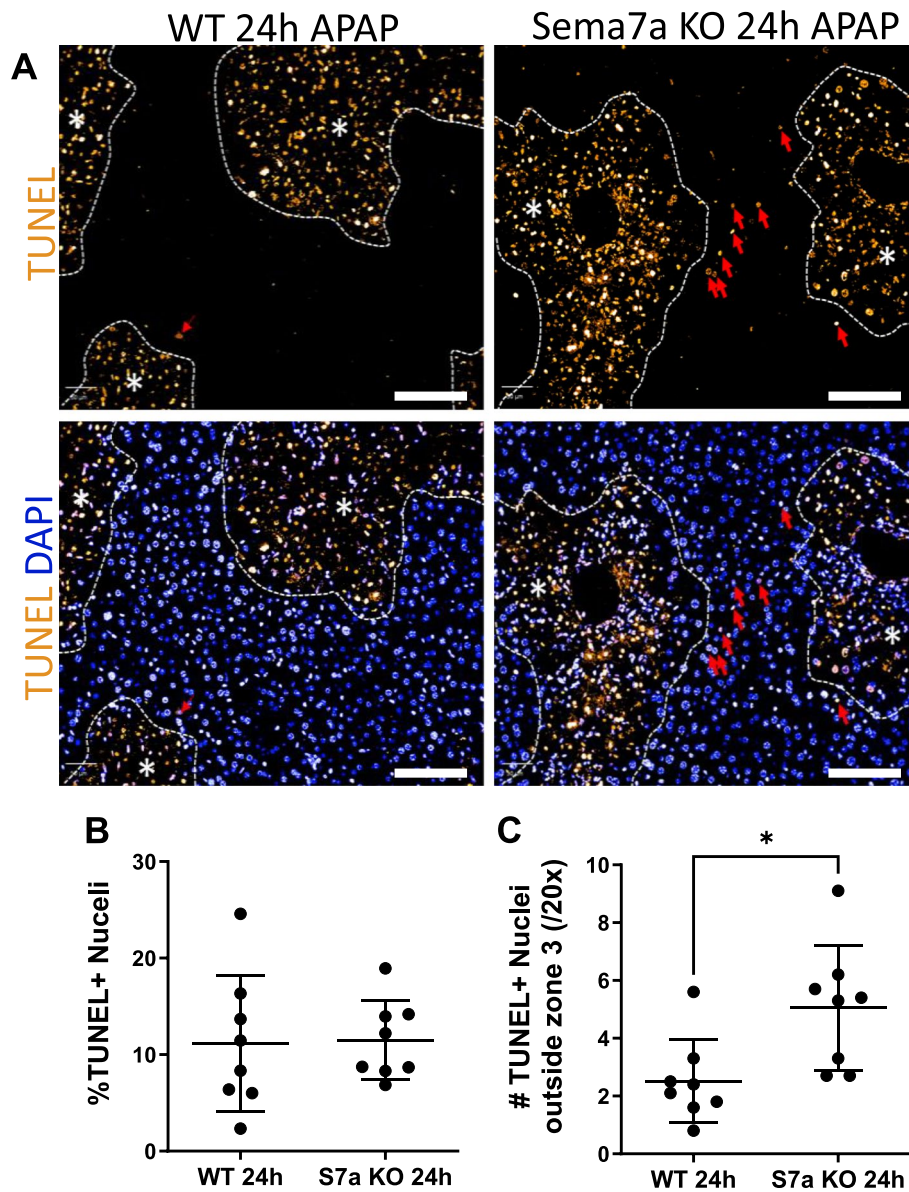


**Fig. 7** Absence of Sema7a on peri-necrotic hepatocytes results in diffuse cell death during APAP-ALI. **A** TUNEL assay (yellow), DAPI (blue), in Sema7a WT and Sema7a KO mice 24 h post APAP-ALI. Necrotic areas outlined with white lines and \*. Red arrows are TUNEL+ nuclei outside the necrotic area. **B** Percentage of TUNEL+DAPI+ nuclei per FOV. **C** Number of TUNEL+DAPI+ nuclei outside the necrotic area, per FOV (t-test,  $p=0.0151$ ). FOV, fields of view. Scale bars 100  $\mu\text{m}$ . Each datapoint represents a mouse.  $n=8$  mice/group. \* $p<0.05$ , \*\* $p<0.01$

$p=0.007$ , respectively) (Fig. 2D), and circulating Sema7a correlated with a serum marker of hepatocellular injury, alanine aminotransferase (ALT) (Pearson coefficient ( $r$ )=0.728, Fig. 2E).

As Sema7a is localised to peri-necrotic hepatocytes, we ensured Sema7a does not label dying cells. Sema7a+hepatocytes are negative for both active caspase 3 and TUNEL+DAPI+nuclei (Supplementary Fig. 1) demonstrated by serial stained sections. Therefore, Sema7a is expressed by the viable hepatocytes, which surround necrosis.

#### Sema7a expressing hepatocytes directly contact cells expressing Sema7a receptors

The predominant Sema7a receptors are Integrin  $\beta 1$  and Plexin C1. Integrin  $\beta 1$  is ubiquitously expressed across the liver [45] and Plexin C1 is expressed by hepatic stellate cells (HSCs), (Supplementary Fig. 2). Integrin  $\beta 1$  is upregulated by HSCs during fibrosis and Sema7a binding is known to contribute to TGF-beta mediated fibrosis [16]. Sema7a also effects spiny stellate cell function [46], but the impact of APAP-ALI on Sema7a receptor expression and their proximity to Sema7a expressing

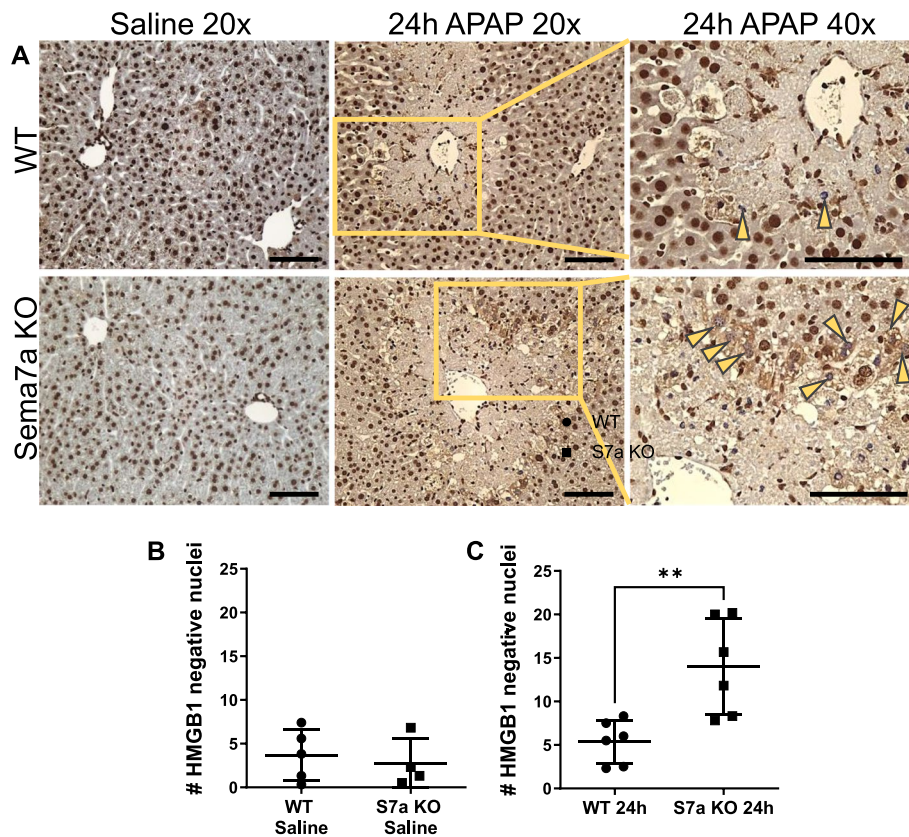


**Fig. 8** Absence of *Sema7a* on peri-necrotic hepatocytes results in higher cell stress during APAP-ALI. Results from WT and *Sema7a* KO mice 24 h post saline or 350 mg/kg APAP. **A** Representative HMGB1 (DAB) labelled hepatic sections from *Sema7a* WT (top) and *Sema7a* KO (bottom) mice with indicated treatments. Inset, area for 40x. Yellow arrowheads, show HMGB1 negative nuclei. **B** Average number of HMGB1- nuclei per FOV quantified in healthy mice. **C** Average number of HMGB1- nuclei per FOV following APAP-ALI were higher in *Sema7a* KO mice (t-test,  $p=0.0058$ ). FOV, fields of view. Scale bars 100  $\mu$ m. Each datapoint represents a mouse.  $n \geq 4$  mice/group,  $**p < 0.01$

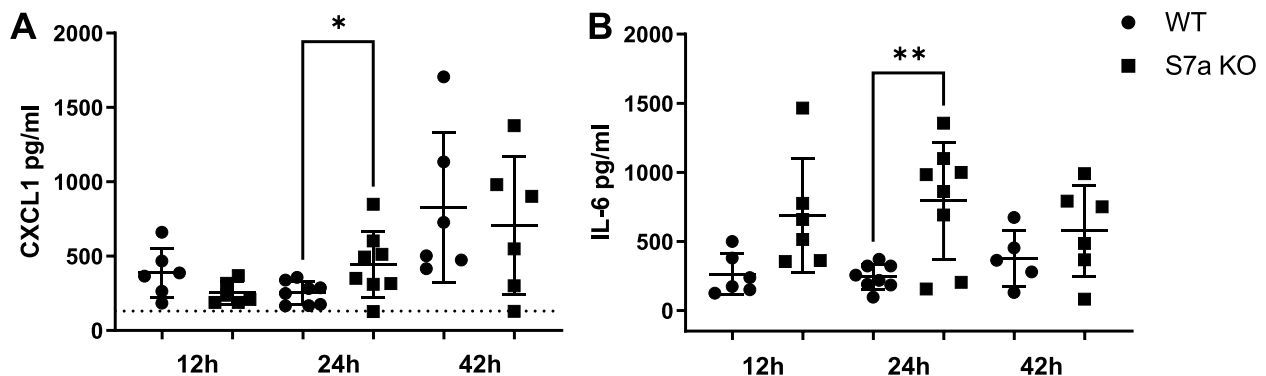


**Fig. 9** *Sema7a* KO mice have increased serum pro-inflammatory cytokines. Serum cytokines in *Sema7a* WT and *Sema7a* KO mice following 350 mg/kg APAP. **A** CXCL1, a neutrophil chemoattractant, was higher in *Sema7a* KO mice serum at 24 h (t-test, Welch's correction,  $p=0.0459$ ). **B** IL-6 was higher in *Sema7a* KO mice serum at 24 h (t-test, Welch's correction,  $p=0.0078$ )

hepatocytes is unknown. To assess this relationship, we completed a dual stain for *Sema7a* during APAP-ALI. Integrin  $\beta 1$ + and Plexin C1+HSCs were detected between the *Sema7a*+hepatocytes at peak *Sema7a*

expression, suggesting a localised signalling interaction (Fig. 3A&B). At 24 h post APAP-ALI, hepatic Integrin  $\beta 1$  mRNA expression and Plexin C1 protein expression increased compared to healthy mice (Supplementary

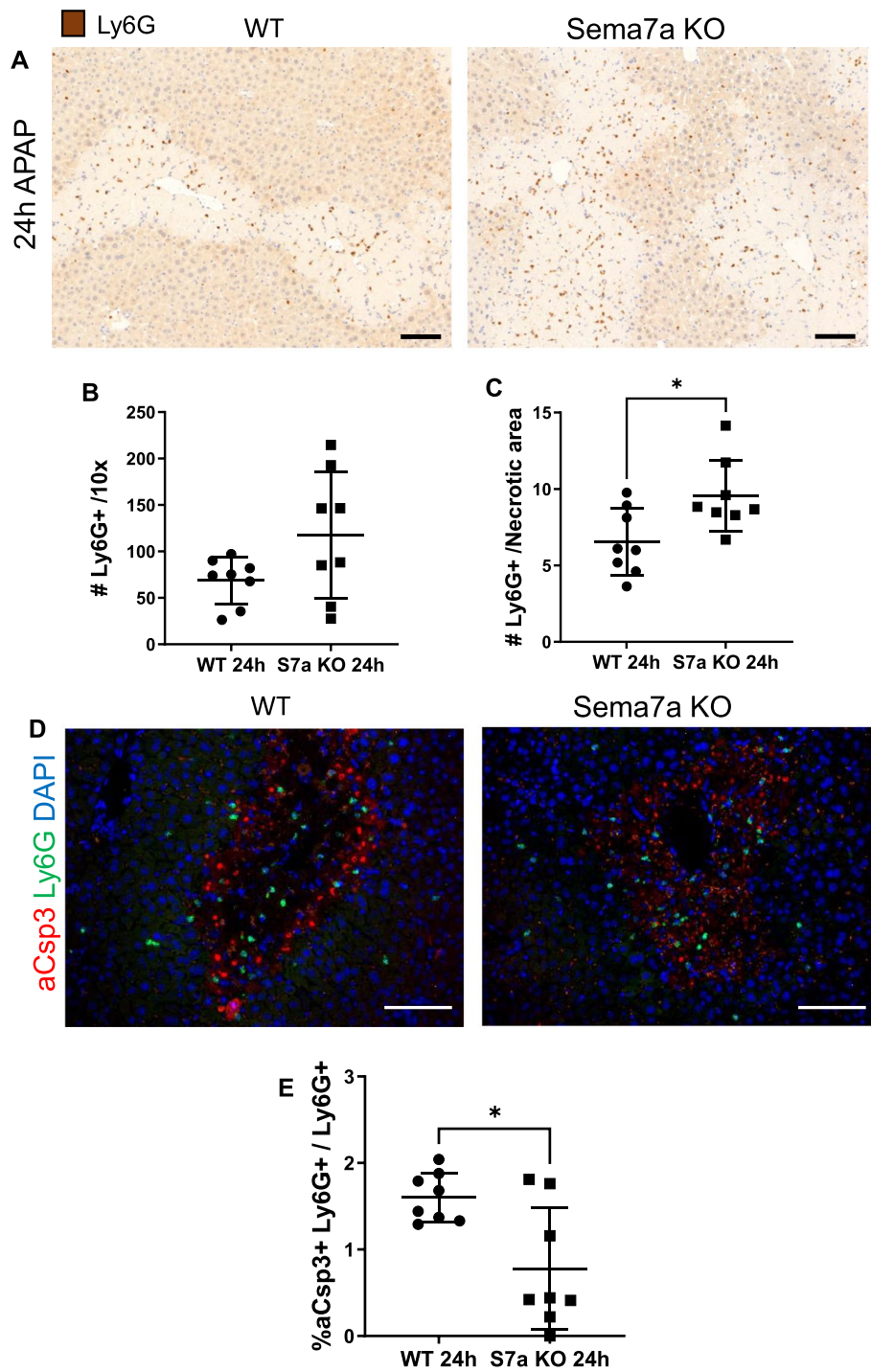


**Fig. 10** Sema7a KO mice have increased neutrophils infiltrating necrotic areas. Results from Sema7a WT and Sema7a KO mice 24 h post 350 mg/kg APAP. **A** Representative Ly6G labelled hepatic sections in Sema7a WT (left) and Sema7a KO mice (right). **B** Average number of Ly6G neutrophils per FOV. **C** The average number of neutrophils within necrosis was higher in Sema7a KO mice (t-test,  $p=0.0182$ ). **D** Ly6G (green) and active Caspase 3 (aCsp3, red) expression in WT (centre) and Sema7a KO mice (right) at 24 h post-APAP-ALI. Quantified (right) as percentage of apoptotic neutrophils (aCsp3+, Ly6G+) in the total Ly6G population. Unpaired t test with Welch's correction,  $p=0.0129$ . Scale bars 100  $\mu$ m. Each datapoint represents a mouse. Unpaired t-test, unless stated. \* $p<0.05$ , \*\* $p<0.01$

Fig. 3). In *Sema7a* KO mice, Plexin C1 but not Integrin  $\beta 1$  expression was reduced at 24 h post APAP (Supplementary Fig. 4,  $p=0.0208$ ), suggesting *Sema7a* promotes the expression of Plexin C1.

#### **Sema7a KO mice have more liver injury during APAP-ALI**

To investigate the importance of peri-necrotic hepatocyte *Sema7a* expression in APAP-ALI we completed experiments in *Sema7a* KO mice. We first confirmed deficiency of *Sema7a* expression in *Sema7a* KO mice both with hepatic qPCR analysis and immunohistochemistry at 24 h post APAP-ALI (Fig. 4). We also compared LFTs, and liver histology (Fig. 5A-C. & Supplementary Fig. 5) of healthy WT and *Sema7a* KO mice and showed no significant differences compared to WT mice (Fig. 5A-C. & Supplementary Fig. 5).

Comparing *Sema7a* KO and WT mice during a time course of 350 mg/kg APAP-ALI identified that *Sema7a* KO mice exhibit significantly more hepatic necrosis at 12 h post APAP-ALI (Fig. 5D-E,  $p=0.0391$ ). This was supported by higher serum ALT ( $p=0.0095$ ) and aspartate aminotransferase (AST) ( $p=0.0107$ , Fig. 6A&B) at 12 h post APAP-ALI. Although increased necrosis was not evident at 24 h post APAP-ALI and only a trended increase was present in LFTs, *Sema7a* KO mice had higher serum bilirubin at 24 h, which can increase with reduced liver function, ( $p=0.0109$ , Supplementary Fig. 5).

#### **Absence of Sema7a on peri-necrotic hepatocytes results in diffuse cell death during APAP-ALI**

Alongside the documented elevated hepatocellular injury and necrosis, deficiency of *Sema7a* in peri-necrotic hepatocytes was associated with alterations in cell death distribution. At 24 h post APAP-ALI, during peak *Sema7a* expression, *Sema7a* KO mice had the same percentage of TUNEL+ nuclei as WT mice, but TUNEL+ nuclei were not contained within the centrilobular necrotic areas and there were TUNEL+ cells in the surrounding healthy parenchyma (Fig. 7,  $p=0.0151$ ), suggesting *Sema7a* plays a localised role to limit the extent of liver tissue damage at 24 h post APAP-ALI.

To further assess if *Sema7a* KO mice have more local tissue inflammation and cell stress during APAP-ALI, High Mobility Group Box 1 (HMGB1) localisation was examined. In healthy mice, HMGB1 is retained in the

nucleus, but is released from necrotic cells, during injury, therefore non-nuclear or cytosolic HMGB1 is a sign of cell stress [47]. Healthy *Sema7a* WT and *Sema7a* KO mice displayed similar nuclear HMGB1 staining (Fig. 8). However, at 24 h post APAP-ALI, *Sema7a* KO mice had significantly more peri-necrotic hepatocytes with HMGB1 negative nuclei ( $p=0.0058$ , Fig. 8).

#### **Sema7a KO mice have more inflammation during APAP-ALI**

Inflammation is known to contribute to APAP induced injury, and *Sema7a* is known as an immunomodulator, so to start assessing the effect of *Sema7a* deficiency on inflammation during APAP-ALI, a panel of pro-inflammatory cytokines were quantified in the serum of *Sema7a* WT and *Sema7a* KO mice throughout the time course. *Sema7a* KO mice had more CXCL1 ( $p=0.0459$ ) and IL-6 ( $p=0.0078$ ) at 24 h post APAP-ALI (Fig. 9), indicative of a higher systemic pro-inflammatory response.

#### **Sema7a KO mice have more neutrophils within necrosis during APAP-ALI**

HMGB1 and CXCL1 are known neutrophil chemoattractants. We therefore quantified numbers of Ly6G+ neutrophils in liver tissue using both immunohistochemistry (Fig. 10 A-B) and flow cytometry, and in whole blood by flow cytometry. *Sema7a* WT and *Sema7a* KO mice had the same total number of hepatic and circulating neutrophils, throughout the APAP-ALI time course (Fig. 10 A-B, Supplementary Fig. 7–9). However, *Sema7a* KO mice had a greater density of neutrophils within centrilobular necrotic areas at 24 h post APAP-ALI, when *Sema7a* expression was otherwise highest in WT mice (Fig. 10 C;  $p=0.0182$ ). WT mice hepatic neutrophils do not express *Sema7a*, but express both known receptors for *Sema7a*, Plexin C1 and Integrin  $\alpha v \beta 1$  (Supplementary Fig. 10).

Neutrophils rapidly migrate into liver after APAP-ALI [48] and we recently identified hepatic neutrophil cleaved caspase 3 expression is markedly reduced, consistent with increased activation and survival [49]. At 24 h post APAP-ALI, we show only 1.6% of neutrophils expressed active caspase 3 in *Sema7a* WT mice consistent with this finding, and this was significantly lower in *Sema7a* KO mice (0.7%, Fig. 10D-E,  $p=0.0129$ ), indicating less neutrophil apoptosis. Although this reduction is

(See figure on next page.)

**Fig. 11** *Sema7a* KO mice show less F4/80+ macrophages at 12 h APAP-ALI, with aberrant localisation. Results are from WT and *Sema7a* KO mice receiving 350 mg/kg APAP or saline. **A** Representative images of liver F4/80+ macrophages in WT (left) and *Sema7a* KO mice (right) at the indicated timepoints. **B** Average number of F4/80+ macrophages per FOV, (12 h t-test,  $p=0.0315$ ). **C** Average number of F4/80+ macrophages in necrotic areas during the time course of APAP-ALI (12 h t-test,  $p=0.044$ ). **D** Location of F4/80+ macrophages in the necrotic area at 24 h APAP-ALI. The necrotic area was separated into outer and central necrotic zones. Average number of F4/80+ macrophages per necrotic zones was calculated in *Sema7a* WT and *Sema7a* KO mice (12 h t-test,  $p=0.0366$ ). Scale bars 100  $\mu$ m. Each datapoint represents an individual mouse.  $n \geq 6$  mice/group.

\* $p < 0.05$

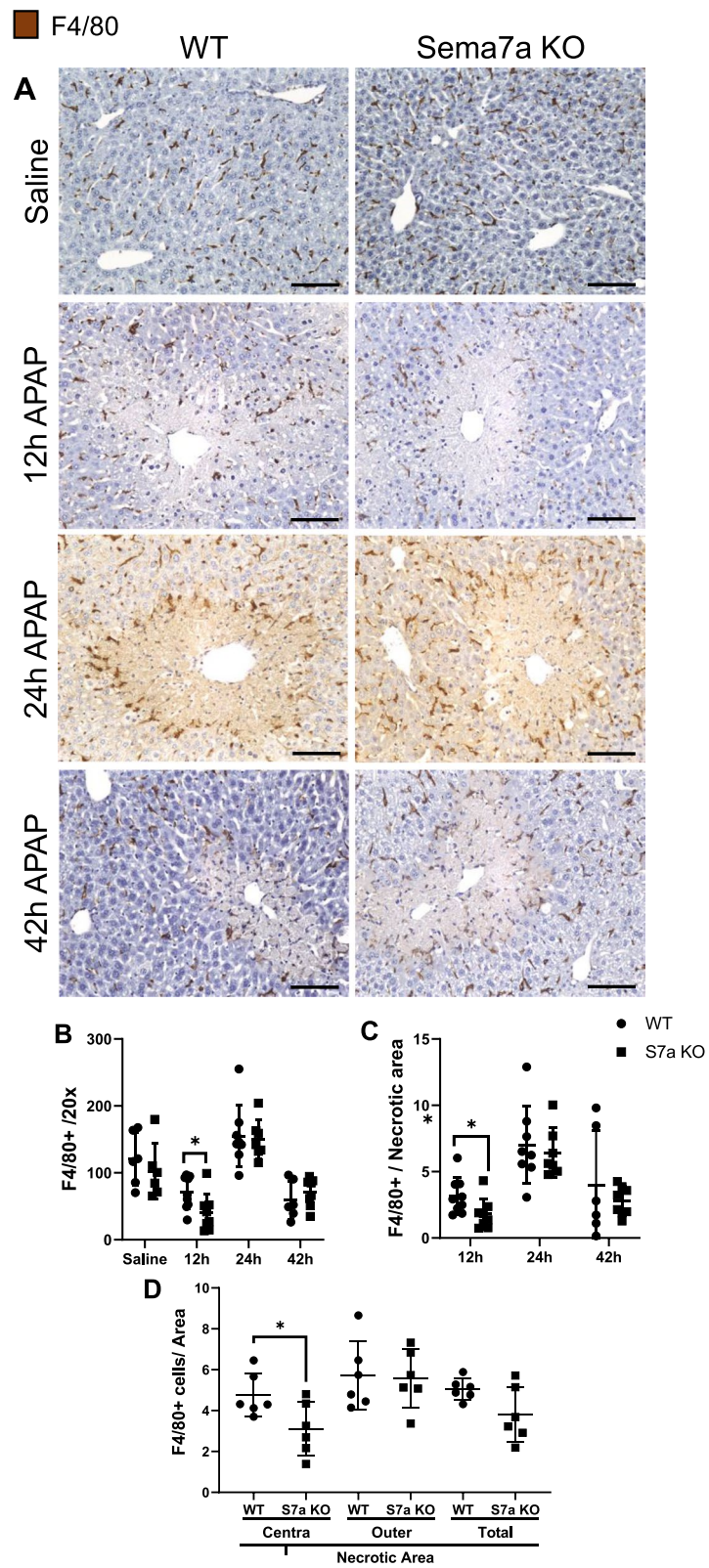


**Fig. 11** (See legend on previous page.)

small, we believe this is significant in this already activated cell population. Further reduction in this marker of cell death could indicate increased neutrophil activation in the *Sema7a* KO mice or altered phagocytosis/clearance of apoptotic neutrophils. Macrophages remove apoptotic neutrophils by phagocytosis [50–53] but this has yet to be shown *in vivo* after APAP-ALI. We investigated the effect of *Sema7a* on phagocytosis with an *in vivo* PKH assay during APAP-ALI and found no differences between *Sema7a* KO and WT mice for monocytes, macrophages, or neutrophils (Supplementary Fig. 11). Therefore, *Sema7a* does not directly impact this form of phagocytosis, though leucocytosis clearance is mediated by *Sema7a* in other models [25].

#### ***Sema7a* KO mice have less F4/80 + macrophages during APAP-ALI**

To examine if a *Sema7a* deficiency impacted liver macrophages, a F4/80 stain was performed (Fig. 11A). Healthy *Sema7a* WT and *Sema7a* KO mice have comparable numbers of F4/80+ macrophages. However, at 12 h post APAP-ALI, total hepatic F4/80+ macrophages numbers were significantly lower in *Sema7a* KO mice ( $p=0.0315$ , Fig. 11B), with a reduced density within the necrotic area ( $p=0.044$ , Fig. 11C) indicating a possible exaggeration of the previously recognised KC depletion [30, 32].

From 12 to 24 h post APAP-ALI the hepatic F4/80+ population increased in both *Sema7a* WT and *Sema7a* mice, consistent with previous literature of infiltrating macrophages replenishing the liver macrophage pool [32]. At 24 h post APAP-ALI total hepatic macrophages were not different (Fig. 11B Supplementary Fig. 12), however, *Sema7a* KO mice had less central necrosis macrophages ( $p=0.0366$ , Fig. 11D), suggesting *Sema7a* has a localised role which facilitates F4/80+ macrophage migration into the necrotic area. During recovery, total hepatic F4/80+ macrophages numbers declined similarly in both *Sema7a* WT and *Sema7a* KO mice (Fig. 11B).

#### **Discussion**

Novel strategies to limit the extent of necrosis, or to promote healthy liver repair from APAP-ALI are urgently required for APAP-overdose patients [2, 5]. Understanding APAP-ALI and secondary inflammation are crucial to identify potential targets for patient therapy. Here, we report a novel role of the immunomodulator *Sema7a* during APAP-ALI.

*Sema7a* is expressed by hepatocytes, shown here and previously [54]. It's highly localised, and increased expression by peri-necrotic hepatocytes during APAP-ALI is a novel finding. Serum concentrations of *Sema7a* correlate with serum injury biomarkers as injury progresses,

consistent with the findings in human paediatric patients with acute inflammatory abdominal disease [26]. *Sema7a* deficiency in this APAP-ALI model was detrimental, leading to increased hepatocellular damage, demonstrated by raised LFTs, more non-nuclear HMGB1 cells, higher necrosis, and TUNEL positivity in liver parenchyma. This finding is in contrast to various non-hepatic models, where *Sema7a* promotes tissue injury and fibrosis [15, 55, 56]. This protective finding is also different to chronic hepatic injury models, such as  $\text{CCl}_4$ -induced liver injury, where *Sema7a* promotes hepatic fibrosis and *Il6* and *Ccl2* expression [16]. More recent hepatobiliary focussed publications identified mutations in *Sema7a* causing a gain of function, progressing disease; non-alcoholic fatty liver disease (NAFLD) and intrahepatic cholestasis [54, 57]. Paradoxical to these studies, in acute sepsis and peritonitis, a protective role of *Sema7a* has been identified through immunomodulation [25, 26]. Here we show a protective action of *Sema7a* in ALI that has not previously been recognised.

We identified that Plexin C1 was reduced in *Sema7a* KO mice, at 24 h APAP-ALI (Supplementary Fig. 6), suggesting *Sema7a* promotes Plexin C1 expression on HSCs. This increased expression of receptor Plexin C1 has also been identified in paediatric systemic vasculitis [58]. As both receptors are present on neutrophils this difference may influence their migration and activation.

Alongside higher hepatic injury and altered receptor expression, *Sema7a* KO mice had more inflammation during APAP-ALI with higher CXCL1 and IL-6 at 24 h. This finding also coincided with alterations in inflammatory cell populations, with both reduced central necrotic zone F4/80+ macrophages and higher neutrophils. As *Sema7a* is a macrophage chemoattractant [20], its lack of expression on peri-necrotic hepatocytes may have reduced monocyte derived macrophage migration, which are known to replenish depleted F4/80 macrophages after in APAP-ALI [32, 59].

As well as hepatic necrosis macrophage reduction we identified that *Sema7a* KO resulted in higher necrosis neutrophils. Neutrophils are attracted to the liver during injury by DAMPs, such as passively released HMGB1 [42–44] or cytokines such as CXCL1 [60]. In *Sema7a* KO mice, the hepatic necrotic area neutrophil increase may be due to the documented HMGB1 and CXCL1 elevations increasing local neutrophil migration or retention. Alternatively, increased numbers may be due to increased survival and potentially activation during APAP-induced inflammation [61]. Körner et al. identified *Sema7a* dampened neutrophil recruitment and was crucial for inflammation resolution, including leukocyte clearance in murine peritonitis. Furthermore, *Sema7a* deficiency may also delay neutrophil migration out of the necrotic

tissue, as endothelial *Sema7a* has been shown to facilitate neutrophil transmigration during pulmonary injury, [18, 29]. Further interrogations of how *Sema7a* impacts in vivo neutrophil migration in APAP-ALI are warranted. *Sema7a* promotes extracellular matrix remodelling factors including *Cathepsin S* [56] and neutrophils secrete cathepsins to degrade basement membranes in sterile thermal liver injury, enabling them to exit the damaged tissue [62]. The increased numbers of necrotic area neutrophils may be one of the reasons for higher hepatic necrosis, consistent with a pro-inflammatory role postulated by several authors [21, 42].

The higher hepatic damage in the *Sema7a* KO mice and higher inflammation in this study may also be due to altered immune cell function. Macrophages are highly plastic cells which acquire distinct phenotypes depending on molecular cues in their microenvironment [32, 33] and *Sema7a* is a recognised cue of macrophage and monocyte activity [15, 63]. We did not find evidence of deficiency of innate immune cell PKH phagocytosis, so reduced efferocytosis of hepatic neutrophils, an important component of inflammation resolution [35, 64], is unlikely in APAP-ALI, despite this finding in peritonitis [26]. Therefore, the increased neutrophils in the necrotic area at 24 h APAP-ALI in *Sema7a* KO mice could be a result of reduced macrophage migration [35, 65]. *Sema7a* has been shown as crucial for the resolution of severe inflammation, through polarization of macrophages to a pro-resolving phenotype in acute peritonitis [26]. This would be an important future direction for research of *Sema7a* in acute liver injuries, given the knowledge that restorative Ly6C<sup>lo</sup> macrophages have been shown to be crucial for appropriate liver repair via phagocytosis [35, 36] and secretion of IL-10 to reduce inflammation [28].

## Conclusion

In conclusion, we have identified a novel hepatoprotective role of *Sema7a* in acute liver injury, with associated innate immunity changes, highlighting a potential immunomodulatory role behind this phenotype. Hepatic *Sema7a* expression increased during the injury phase of APAP-ALI and peak expression was localised to the peri-necrotic area. Without peri-necrotic *Sema7a* there was more hepatic necrosis during injury (12 h) and cellular damage (TUNEL+ and HMGB1-) was not restricted to the necrotic region. *Sema7a* deficiency resulted in more inflammation at 24 h post APAP-ALI, with increased IL6 and CXCL1 quantification. There were more neutrophils within necrosis, with lower cleaved caspase 3, indicating increased activation. There were also lower necrotic area macrophages, key cells for liver repair following APAP-ALI. Future work to further clarify the mechanisms

behind the hepatoprotective effect of *Sema7a* in APAP-ALI are warranted. Better understanding of these mechanisms might identify this as a novel therapeutic target to limit the spread of necrosis and reduce inflammation during acute tissue injury.

## Abbreviations

APAP	Acetaminophen
APAP-ALI	Acetaminophen-induced liver injury
ALF	Acute liver failure
ALT	Alanine aminotransferase
APAP-ALI	APAP-induced acute liver injury
AST	Aspartate aminotransferase
CXCL1	Chemokine (C-X-C motif) ligand 1
DAMPs	Danger-associated-molecular patterns
HSCs	Hepatic stellate cells
HMGB1	High mobility group box 1
IL	Interleukin
KCs	Kupffer cells
KO	Knockout
LFTs	Liver function tests
NAC	N-acetylcysteine
NAFLD	Non-alcoholic fatty liver disease
<i>Sema7a</i>	Semaphorin 7a
WT	Wild-type

## Supplementary Information

The online version contains supplementary material available at <https://doi.org/10.1186/s12950-025-00429-x>.

Supplementary Material 1.

## Acknowledgements

We thank F. Rossi and C. Cryer with fluorescence-activated cell sorting (FACS)

## Authors' contributions

Authors' contributions: Conceptualisation and design (E.J.L., J.A.C., L.C., P.S.L., B.J.D., L.B., S.J.F.). Data generation (E.J.L., J.A.C., L.C., P.S.L., R.A., T.-Y.K., M.V.). Data analysis and interpretation (E.J.L., J.A.C., L.C., B.J.D., P.S.L., M.V., L.B., S.J.F., A.G.R.). Manuscript preparation (E.J.L., J.A.C., L.C., P.S.L., S.J.F.). Review and editing (E.J.L., J.A.C., B.J.D., M.V., L.C., P.S.L., S.J.F., A.G.R.). Funding acquisition (S.J.F.).

## Funding

Funding is acknowledged from the MRC Centre for regenerative Medicine PhD Studentship MR/L501426/1 and the Wellcome Trust [108906/Z/15/Z] JAC.

## Data availability

No datasets were generated or analysed during the current study.

## Declarations

### Competing interests

There was no competing interests at the time of experiments, however L.C., B.J.D., and S.J.F. are shareholders of Resolution Therapeutics Ltd. a macrophage cell therapy developer. S.J.F. is a scientific adviser and L.C. is an employee of Resolution Therapeutics.

### Author details

<sup>1</sup>Centre for Regenerative Medicine, Institute for Regeneration and Repair, University of Edinburgh, Edinburgh, UK. <sup>2</sup>Centre for Inflammation Research, Institute for Regeneration and Repair, University of Edinburgh, Edinburgh, UK. <sup>3</sup>The Royal (Dick) School of Veterinary Studies and The Roslin Institute, University of Edinburgh, Edinburgh, UK. <sup>4</sup>MRC Human Genetics Unit, Institute of Genetics and Molecular Medicine, University of Edinburgh, Edinburgh EH4 2XU, UK.

Received: 4 October 2024 Accepted: 13 January 2025  
Published online: 20 March 2025

## References

- Bernal W, Auzinger G, Dhawan A, Wendon J. Acute liver failure. *The Lancet*. 2010;376:190–201.
- Reuben A, Tillman H, Fontana RJ, Davern T, Mcguire B, Stravitz RT, Durkalski V, Larson AM, Liou I, Fix O, Schilsky M, Mccashland T, Hay JE, Murray N, Shaikh OS, Ganger D, Zaman A, Han SB, Chung RT, Smith A, Brown R, Crippin J, Harrison ME, Koch D, Munoz S, Reddy KR, Rossaro L, Satyanarayana R, Hassanein T, Hanje AJ, Olson J, Subramanian R, Karvellas C, Hameed B, Sherker AH, Robuck P, Lee WM. Outcomes in adults with acute liver failure between 1998 and 2013: An observational cohort study. *Ann Intern Med*. 2016;164:724–32.
- Karvellas CJ, Leventhal TM, Rakela JL, Zhang J, Durkalski V, Reddy KR, Fontana RJ, Stravitz RT, Lake JR, Lee WM, Parekh JR. Outcomes of patients with acute liver failure listed for liver transplantation: A multicenter prospective cohort analysis. *Liver Transpl*. 2023;29:318–30.
- Rolando N, Wade J, Davalos M, Wendon J, Philpott-Howard J, Williams R. The systemic inflammatory response syndrome in acute liver failure. *Hepatology*. 2000;32:734–9.
- Stravitz RT, Fontana RJ, Karvellas C, Durkalski V, Mcguire B, Rule JA, Tujios S, Lee WM. Acute Liver Failure Study Group. Future directions in acute liver failure. *Hepatology* 2023;78:1266–1289.
- Prescott LF, Critchley JAJH, Proudfoot AT, Illingworth RN, Stewart MJ, Adam RD. Intravenous N-acetylcysteine: The treatment of choice for paracetamol poisoning. *Br Med J*. Epub ahead of print 1979. <https://doi.org/10.1136/bmj.2.6198.1097>.
- Lee WM. Acetaminophen (APAP) hepatotoxicity—Isn't it time for APAP to go away? *J Hepatol*. 2017;67:1324–31.
- Simpson KJ, Bates CM, Henderson NC, Wigmore SJ, Garden OJ, Lee A, Pollok A, Masterton G, Hayes PC. The utilization of liver transplantation in the management of acute liver failure: Comparison between acetaminophen and non-acetaminophen etiologies. *Liver Transpl*. 2009;15:600–9.
- Pasterkamp RJ, Peschon JJ, Spriggs MK, Kolodkin AL. Semaphorin 7A promotes axon outgrowth through integrins and MAPKs. *Nature*. 2003;424:398–405.
- Song Y, Wang L, Zhang L, Huang D. The involvement of semaphorin 7A in tumorigenic and immunoinflammatory regulation. *J Cell Physiol*. 2021;236:6235–48.
- Köhler D, Granja T, Volz J, Koeppen M, Langer HF, Hansmann G, Legchenko E, Geisler T, Bakchoui T, Eggstein C, Häberle HA, Nieswandt B, Rosenberger P. Red blood cell-derived semaphorin 7A promotes thrombo-inflammation in myocardial ischemia-reperfusion injury through platelet GPIb. *Nat Commun*;11. Epub ahead of print December 1, 2020. <https://doi.org/10.1038/s41467-020-14958-x>.
- Carulli D, de Winter F, Verhaagen J. Semaphorins in Adult Nervous System Plasticity and Disease. *Frontiers in Synaptic Neuroscience*;13. Epub ahead of print May 11, 2021. <https://doi.org/10.3389/fnsyn.2021.672891>.
- Nishide M, Kumanogoh A. The role of semaphorins in immune responses and autoimmune rheumatic diseases. *Nat Rev Rheumatol*. 2018;14:19–31.
- Worzfeld T, Offermanns S. Semaphorins and plexins as therapeutic targets. *Nat Rev Drug Discov*. 2014;13:603–21.
- Suzuki K, Okuno T, Yamamoto M, Pasterkamp RJ, Takegahara N, Takamatsu H, Kitao T, Takagi J, Rennert PD, Kolodkin AL, Kumanogoh A, Kikutani H. Semaphorin 7A initiates T-cell-mediated inflammatory responses through alpha1beta1 integrin. *Nature*. 2007;446:680–4.
- De Minicis S, Rychlicki C, Agostinelli L, Saccomanno S, Trozzi L, Candelaresi C, Battaller R, Millán C, Brenner D a., Vivarelli M, Mocchegiani F, Marziani M, Benedetti A, Svegliati-Baroni G. Semaphorin 7A contributes to TGF-β-mediated liver fibrogenesis. *Am J Pathol* 2013;183:820–30.
- Liu H, Juo ZS, Shim AHR, Focia PJ, Chen X, Garcia KC, He X. Structural Basis of Semaphorin-Plexin Recognition and Viral Mimicry from Sema7A and A39R Complexes with PlexinC1. *Cell*. 2010;142:749–61.
- Morote-Garcia JC, Napiwotzky D, Köhler D, Rosenberger P, Kohler D, Rosenberger P, Köhler D, Rosenberger P, Kohler D, Rosenberger P, Köhler D, Rosenberger P, Kohler D, Rosenberger P. Endothelial Semaphorin 7A promotes neutrophil migration during hypoxia. *Proc Natl Acad Sci U S A*. 2012;109:14146–51.
- Granja T, Köhler D, Mirakaj V, Nelson E, König K, Rosenberger P. Crucial role of Plexin C1 for pulmonary inflammation and survival during lung injury. *Mucosal Immunol*. 2014;7:879–91.
- Elder AM, Tamburini BAJ, Crump LS, Black SA, Wessells VM, Schedin PJ, Borges VF, Lyons TR. Semaphorin 7A promotes macrophage-mediated lymphatic remodeling during postpartum mammary gland involution and in breast cancer. *Cancer Res*. 2018;78:6473–85.
- Holmes S, Downs AM, Fosberry A, Hayes PD, Michalovich D, Murdoch P, Moores K, Fox J, Deen K, Pettman G, Wattam T, Lewis C. Sema7A is a potent monocyte stimulator. *Scand J Immunol*. 2002;56:270–5.
- Kang S, Okuno T, Takegahara N, Takamatsu H, Nojima S, Kimura T, Yoshida Y, Ito D, Ohmae S, You D-J, Toyofuku T, Jang MH, Kumanogoh A. Intestinal epithelial cell-derived semaphorin 7A negatively regulates development of colitis via αvβ1 integrin. *J Immunol*. 2012;188:1108–16.
- Mizutani N, Nabe T, Yoshino S. Semaphorin 7A plays a critical role in IgE-mediated airway inflammation in mice. *Eur J Pharmacol*. 2015;764:149–56.
- Chen X, Wang H, Jia K, Wang H, Ren T. Anti-Semaphorin-7A single chain antibody demonstrates beneficial effects on pulmonary inflammation during acute lung injury. *Exp Ther Med*. 2018;15:2356–64.
- Körner A, Köhler D, Schneider M, Roth JM, Granja TF, Eggstein C, Mirakaj V, Rosenberger P. Semaphorin 7A is protective during inflammatory peritonitis through integrin receptor signaling. *Front Immunol*;14. Epub ahead of print 2023. <https://doi.org/10.3389/fimmu.2023.1251026>.
- Körner A, Bernard A, Fitzgerald JC, Alarcon-Barrera JC, Kostidis S, Kaussen T, Giera M, Mirakaj V. Sema7A is crucial for resolution of severe inflammation. *Proc Natl Acad Sci*. 2021;118: e2017527118.
- Laskin DL, Gardner CR, Price VF, Jollow DJ. Modulation of macrophage functioning abrogates the acute hepatotoxicity of acetaminophen. *Hepatology*. 1995;21:1045–50.
- Ju C, Reilly TP, Bourdi M, Radonovich MF, Brady JN, George JW, Pohl LR. Protective role of kupffer cells in acetaminophen-induced hepatic injury in mice. *Chem Res Toxicol*. 2002;15:1504–13.
- You Q, Holt M, Yin H, Li G, Hu CJ, Ju C. Role of hepatic resident and infiltrating macrophages in liver repair after acute injury. *Biochem Pharmacol*. 2013;86:836–43.
- Mossanen JC, Krenkel O, Ergen C, Govaere O, Liepelt A, Puengel T, Heymann F, Kalthoff S, Lefebvre E, Eulberg D, Luedde T, Marx G, Strassburg CP, Roskams T, Trautwein C, Tacke F. Chemokine (C-C motif) receptor 2-positive monocytes aggravate the early phase of acetaminophen-induced acute liver injury. *Hepatology*;64. Epub ahead of print 2016. <https://doi.org/10.1002/hep.28682>.
- Moore JK, MacKinnon AC, Man TY, Manning JR, Forbes SJ, Simpson KJ. Patients with the worst outcomes after paracetamol (acetaminophen)-induced liver failure have an early monocytopenia. *Aliment Pharmacol Ther*. 2017;45:443–54.
- Zigmond E, Samia-Grinberg S, Pasmanik-Chor M, Brazowski E, Shibolet O, Halpern Z, Varol C. Infiltrating Monocyte-Derived Macrophages and Resident Kupffer Cells Display Different Ontogeny and Functions in Acute Liver Injury. *J Immunol*. 2014;193:344–53.
- Wen Y, Lambrecht J, Ju C, Tacke F. Hepatic macrophages in liver homeostasis and diseases—diversity, plasticity and therapeutic opportunities. *Cell Mol Immunol*. 2021;18:45–56.
- Ramachandran P, Pellicoro A, Vernon MA, Boulter L, Aucott RL, Ali A, Hartland SN, Snowden VK, Cappon A, Gordon-Walker TT, Williams MJ, Dunbar DR, Manning JR, Van Rooijen N, Fallowfield JA, Forbes SJ, Iredale JP. Differential Ly-6C expression identifies the recruited macrophage phenotype, which orchestrates the regression of murine liver fibrosis. *Proc Natl Acad Sci U S A*;109. Epub ahead of print 2012. <https://doi.org/10.1073/pnas.1119964109>.
- Triantafyllou E, Pop OT, Possamai LA, Wilhelm A, Liaskou E, Singanayagam A, Bernsmeier C, Khamri W, Petts G, Dargue R, Davies SP, Tickle J, Yuksel M, Patel VC, Abeles RD, Stamataki Z, Curbishley SM, Ma Y, Wilson ID, Coen M, Woollard KJ, Quaglia A, Wendon J, Thurst MR, Adams DH, Weston CJ, Antoniaades CG. MerTK expressing hepatic macrophages promote the resolution of inflammation in acute liver failure. *Gut*. 2018;67:333–47.
- Campana L, Starkey Lewis PJ, Pellicoro A, Aucott RL, Man J, O'Duibhir E, Mok SE, Ferreira-Gonzalez S, Livingstone E, Greenhalgh SN, Hull KL, Kendall TJ, Vernimmen D, Henderson NC, Boulter L, Gregory CD, Feng Y, Anderton SM, Forbes SJ, Iredale JP. The STAT3–IL-10–IL-6 Pathway Is a

